

A novel one-dimensional nickel(II) alternating chain from discrete pyrazolate-based dinuclear complexes

Franc Meyer,^{*,†,a} Uwe Ruschewitz,^b Peter Schober,^a Björn Antelmann^a and Laszlo Zsolnai^a

^a Anorganisch-Chemisches Institut der Universität Heidelberg, Im Neuenheimer Feld 270, D-69120 Heidelberg, Germany

^b Institut für Anorganische Chemie der RWTH Aachen, Prof.-Pirlet-Straße 1, D-52056 Aachen, Germany

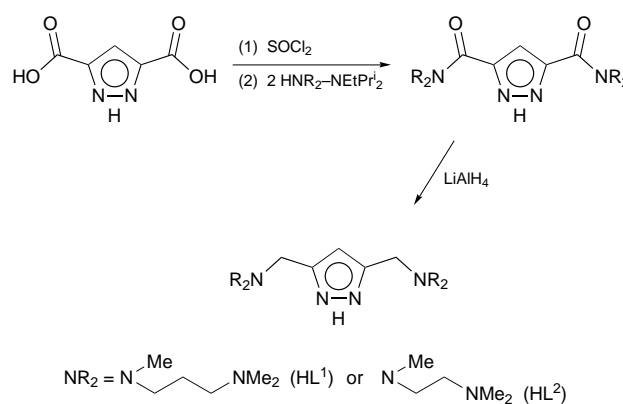
Hexadentate dinucleating ligands that are based on a bridging pyrazolate bearing chelating side arms [3,5-(R₂NCH₂)₂C₃N₂H₂; R₂N = Me₂N(CH₂)₃NMe (HL¹), Me₂N(CH₂)₂NMe (HL²)] reacted with NiCl₂·6H₂O to yield complexes ClNi(μ-Cl)(μ-L¹)NiCl **1** (Ni₂L¹Cl₃) and ClNi(μ-Cl)(μ-L²)NiCl **2** (Ni₂L²Cl₃), respectively. Depending on the side-arm chain length and the solvent used for crystallisation these complexes either crystallised as discrete bimetallic units (**1**) or were assembled *via* di-μ-chloro linkages to form a tetranuclear compound [ClNi(μ-Cl)(μ-L²)Ni(μ-Cl)₂Ni(μ-Cl)(μ-L²)NiCl] **2a** ([Ni₂L²Cl₃]₂) or a novel bridge-alternating one-dimensional chain [Ni(μ-Cl)(μ-L¹)Ni(μ-Cl)]_∞ **2b** ([Ni₂L²Cl₃]_∞) in the solid state. Variable-temperature magnetic susceptibility measurements revealed antiferromagnetic coupling within the basic μ-chloro-μ-pyrazolato bridged bimetallic framework in all cases and also suggested antiferromagnetic superexchange propagated by the di-μ-chloro linkage in **2b**. The latter result is rationalised on the basis of the specific geometric findings for this di-μ-chloro linkage, in particular the unusually large Ni–Cl–Ni angle [101.37(4)°].

In the last decade much research has been devoted to the study of magnetic interactions between paramagnetic centres in exchange-coupled systems.^{1,2} Thereby the interest has extended from dinuclear to oligonuclear and polymeric compounds, and some of the more recent work in low-dimensional magnetism has focused on one-dimensional exchange-alternating linear chains with local spins $S > \frac{1}{2}$.^{3–5} The theoretical treatment of the *J*-alternating $S = 1$ chain by Borrás-Almenar and co-workers⁶ strongly stimulated experimental searches for systems of this kind, however fully characterised examples have still remained rare^{3,4,7} and in most cases are derived from the co-ordinative versatility of the multidentate azido ligand.^{4,8} While the general and most often pursued synthetic strategy, *i.e.* the mixing of an appropriate metal salt with different types of potential ligands, leaves the formation of the desired alternating one-dimensional system to the whims of nature, a more systematic approach is based on the linking of discrete bimetallic complexes with accessible co-ordination sites.⁷ We recently described the synthesis and co-ordination potential of a series of dinucleating pyrazolate ligands with chelating polyamino substituents in the 3- and 5-positions of the heterocycle,⁹ where characteristic features of the resulting metal complexes like the metal–metal separation or co-ordination numbers can be selectively tuned by varying the side arm chain length¹⁰ and donor types.¹¹ In the present contribution we employ bimetallic systems of this kind to construct a novel one-dimensional $S = 1$ alternating chain from the assembly of basic dinickel(II) entities. Ligands L¹ and L² (Scheme 1) were chosen in order to provide fewer donor sites than required to co-ordinatively saturate a nickel(II) ion in each co-ordination compartment and thus allow for the requisite linking of the pyrazolate-based dinuclear complexes.

Results and Discussion

Syntheses and general characterisation

The new ligand HL² is synthesised analogously to the preparation of HL¹ reported previously⁹ (Scheme 1). Thus pyrazole-



Scheme 1

3,5-dicarboxylic acid is converted into the corresponding bis(amide) by treatment with SOCl₂¹² and subsequent reaction with the appropriate secondary amine in the presence of NEtPr₂. The resulting bis(amide) can then be reduced using an excess of LiAlH₄ to yield the polydentate ligand HL² as a slightly yellowish oil.

For the synthesis of nickel(II) complexes the potential ligands HL¹ and HL² are treated with 2 equivalents of NiCl₂·6H₂O in the presence of NEtPr₂ to afford green solutions of co-ordination compounds Ni₂L¹Cl₃ **1** and Ni₂L²Cl₃ **2**, whose formations are corroborated by elemental analyses and by the FAB-MS spectra. Although no definite conclusions can be drawn from the solution UV/VIS spectra (Table 1), the ligand-field transitions observed for **1** and **2** bear close resemblance with those observed for complexes containing five-co-ordinate high spin Ni^{II} ions.¹³ As expected, the band positions for **2** in CH₂Cl₂ and in CHCl₃ are very similar, indicating the presence of identical five-co-ordinate dinuclear Ni^{II} species in solution, in contrast to the different solid-state structures obtained by crystallisation from these two solvents (see below). A solid-state UV/VIS spectrum of the green crystals of **2** obtained from CH₂Cl₂–light petroleum (b.p. 40–60 °C) reveals three absorptions that differ significantly from the solution data, but are

† E-Mail: Franc@sun0.urz.uni-heidelberg.de

Table 1 The UV/VIS data of the complexes

	$\tilde{\nu}/\text{cm}^{-1}$ ($\epsilon/\text{M}^{-1}\text{cm}^{-1}$)
1 ^a	13 660 (80), 23 640 (240)
2 ^a	12 990 (60), 22 270 (120)
2 ^b	13 070 (60), 22 320 (140)
2b ^c	8370 [ν_1], 14 300 [ν_2], 23 750 [ν_3]

^a In CHCl_3 , ^b In CH_2Cl_2 , ^c Powder in Nujol.

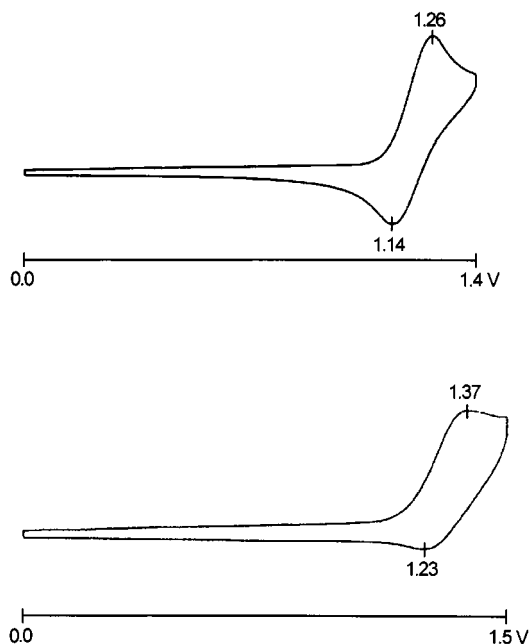


Fig. 1 Cyclic voltammograms of complexes **1** (top) and **2** (bottom) in CH_2Cl_2 containing NBu_4PF_6 (0.1 M) at scan speed 200 mV s^{-1}

typical for a d^8 ion in a near-octahedral co-ordination sphere,^{13c} i.e. they are assigned to spin-allowed transitions from $^3A_{2g}$ to $^3T_{2g}$, $^3T_{1g}(\text{F})$ and $^3T_{1g}(\text{P})$, respectively (Table 1).

Both complexes **1** and **2** have been studied by cyclic voltammetry in the potential range 0.0 to 1.50 V vs. SCE in CH_2Cl_2 (Fig. 1). Complex **1** shows a reversible oxidation wave at $E_2 = +1.26\text{ V}$ ($\Delta E = E_{\text{pc}} - E_{\text{pa}} = 120\text{ mV}$ at scan speed 200 mV s^{-1}), presumably corresponding to the formation of a mixed-valence $\text{Ni}^{\text{III}}\text{Ni}^{\text{II}}$ compound. In contrast, the cyclic voltammogram of **2** displays an oxidation process at $E_{\text{p}}^{\text{ox}} = +1.37\text{ V}$ (200 mV s^{-1}) that is irreversible at low scan rates but changes its shape with increasing scan rates to become quasi-reversible and yields $E_2 = 1.33\text{ V}$ ($\Delta E = 200\text{ mV}$ at scan rate 800 mV s^{-1}). It thus transpires that the longer and more flexible ligand side arms in **1** are more favourable for the adaptation to an oxidised $\text{Ni}^{\text{III}}\text{Ni}^{\text{II}}$ species than the smaller sized chelate rings enforced by the shorter side arms in **2**.

Description of the solid-state structures

Complex **1** crystallises in the orthorhombic space group $Pbca$ with two CHCl_3 solvent molecules per bimetallic entity in the unit cell. Selected bond distances and angles are given in Table 2, the molecular structure is depicted in Fig. 2. It shows discrete dinuclear molecules in which two nickel ions are bridged by both the pyrazolate of the primary ligand L^1 and a chlorine atom. Each nickel centre is found to be five-co-ordinate in an approximately square pyramidal co-ordination environment with the outermost nitrogen donors N(4) and N(6) in the apical positions. The structure of **1** is thus very similar to those of a related cobalt(II) compound reported previously.⁹ Interestingly, the species $\text{Ni}_2\text{L}^2\text{Cl}_3$ yields orange-yellow crystals (**2a**) when a solution of the complex in CHCl_3 is layered with light petroleum, but green crystals (**2b**) from the CH_2Cl_2 -light petroleum

Table 2 Selected bond distances (\AA) and angles ($^\circ$) for complex **1**

Ni(1)–N(1)	1.959(6)	Ni(2)–N(5)	2.182(6)
Ni(1)–N(3)	2.163(6)	Ni(2)–N(6)	2.068(6)
Ni(1)–N(4)	2.074(6)	Ni(2)–Cl(2)	2.439(2)
Ni(1)–Cl(1)	2.292(2)	Ni(2)–Cl(3)	2.294(2)
Ni(1)–Cl(2)	2.445(2)	N(1)–N(2)	1.365(8)
Ni(2)–N(2)	1.961(6)	Ni(1)⋯Ni(2)	3.918
N(1)–Ni(1)–N(3)	78.8(2)	N(2)–Ni(2)–Cl(2)	86.1(2)
N(1)–Ni(1)–N(4)	107.7(2)	N(2)–Ni(2)–Cl(3)	154.2(2)
N(1)–Ni(1)–Cl(1)	153.4(2)	N(5)–Ni(2)–N(6)	94.9(2)
N(1)–Ni(1)–Cl(2)	85.4(2)	N(5)–Ni(2)–Cl(2)	159.9(2)
N(3)–Ni(1)–N(4)	94.5(2)	N(5)–Ni(2)–Cl(3)	95.5(2)
N(3)–Ni(1)–Cl(1)	96.2(2)	N(6)–Ni(2)–Cl(2)	102.0(2)
N(3)–Ni(1)–Cl(2)	159.8(2)	N(6)–Ni(2)–Cl(3)	99.1(2)
N(4)–Ni(1)–Cl(1)	98.7(2)	Cl(2)–Ni(2)–Cl(3)	92.6(1)
N(4)–Ni(1)–Cl(2)	102.2(2)	Ni(1)–N(1)–N(2)	131.5(4)
Cl(1)–Ni(1)–Cl(2)	92.4(1)	Ni(2)–N(2)–N(1)	129.8(4)
N(2)–Ni(2)–N(5)	78.6(2)	Ni(1)–Cl(2)–Ni(2)	106.7(1)
N(2)–Ni(2)–N(6)	106.3(3)		

Table 3 Selected bond distances (\AA) and angles ($^\circ$) for complex **2a**

Ni(1)–N(1)	1.987(3)	Ni(2)–N(5)	2.246(3)
Ni(1)–N(3)	2.205(3)	Ni(2)–N(6)	2.066(3)
Ni(1)–N(4)	2.182(3)	Ni(2)–Cl(2)	2.435(1)
Ni(1)–Cl(1)	2.567(1)	Ni(2)–Cl(3)	2.275(1)
Ni(1)–Cl(1 ¹)	2.378(1)	N(1)–N(2)	1.349(4)
Ni(1)–Cl(2)	2.536(1)	Ni(1)⋯Ni(2)	3.924
Ni(2)–N(2)	1.950(3)	Ni(1)⋯Ni(1 ¹)	3.774
N(1)–Ni(1)–N(3)	78.3(1)	N(2)–Ni(2)–N(5)	77.5(1)
N(1)–Ni(1)–N(4)	97.0(1)	N(2)–Ni(2)–N(6)	105.2(1)
N(1)–Ni(1)–Cl(1)	88.84(9)	N(2)–Ni(2)–Cl(2)	88.64(9)
N(1)–Ni(1)–Cl(1 ¹)	169.09(8)	N(2)–Ni(2)–Cl(3)	147.02(9)
N(1)–Ni(1)–Cl(2)	85.20(8)	N(5)–Ni(2)–N(6)	84.7(1)
N(3)–Ni(1)–N(4)	83.1(1)	N(5)–Ni(2)–Cl(2)	165.36(8)
N(3)–Ni(1)–Cl(1)	91.10(8)	N(5)–Ni(2)–Cl(3)	99.08(8)
N(3)–Ni(1)–Cl(1 ¹)	99.22(8)	N(6)–Ni(2)–Cl(2)	94.74(9)
N(3)–Ni(1)–Cl(2)	159.70(8)	N(6)–Ni(2)–Cl(3)	107.11(9)
N(4)–Ni(1)–Cl(1)	170.77(8)	Cl(2)–Ni(2)–Cl(3)	95.07(4)
N(4)–Ni(1)–Cl(1 ¹)	93.22(8)	Ni(1)–N(1)–N(2)	131.8(2)
N(4)–Ni(1)–Cl(2)	87.35(8)	Ni(2)–N(2)–N(1)	129.3(2)
Cl(1)–Ni(1)–Cl(1 ¹)	80.57(4)	Ni(1)–Cl(2)–Ni(2)	104.23(4)
Cl(1)–Ni(1)–Cl(2)	100.31(4)	Ni(1)–Cl(1)–Ni(1 ¹)	99.43(4)
Cl(1 ¹)–Ni(1)–Cl(2)	99.18(4)		

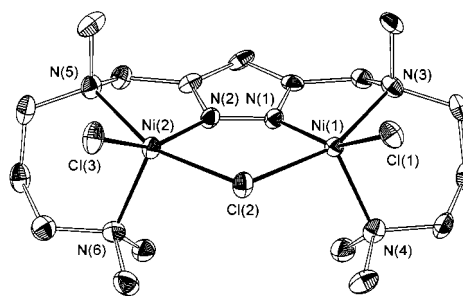


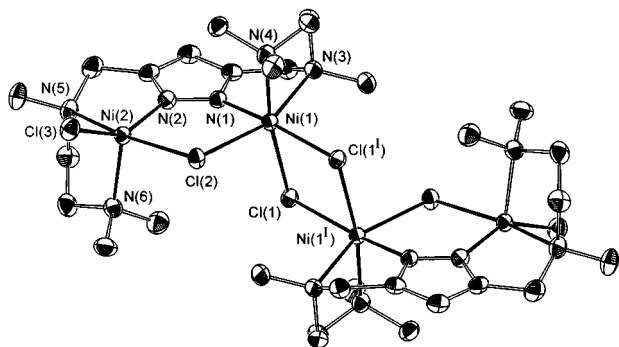
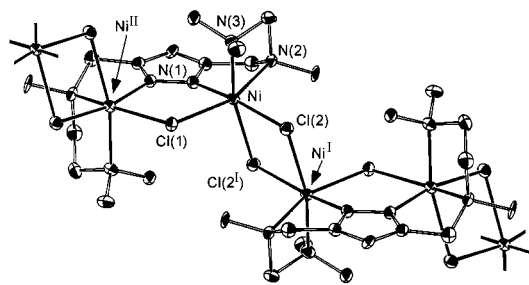
Fig. 2 View of the molecular structure of complex **1** (30% probability ellipsoids). In the interests of clarity all hydrogen atoms have been omitted

solvent system. In the former case the complex crystallises in the triclinic space group $P\bar{1}$ with two CHCl_3 solvent molecules per pyrazolate-based dinickel unit. The molecular structure of **2a** is shown in Fig. 3, selected bond lengths and angles are listed in Table 3.

The structural analysis shows that two pyrazolate-based bimetallic entities similar to **1** are dimerised *via* two chlorine atoms to form linear tetranuclear species containing two six-co-ordinate nickel(II) ions in a distorted octahedral surrounding, that are flanked by terminal five-co-ordinate nickel(II) ions intermediate between *SPY-5* (square pyramidal) and *TBPY-5*

Table 4 Selected bond distances (Å) and angles (°) for complex **2b**

Ni–N(1)	1.979(4)	Ni–Cl(2 ^I)	2.592(1)
Ni–N(2)	2.197(4)	N(1)–N(1 ^{II})	1.385(7)
Ni–N(3)	2.160(4)	Ni···Ni ^I	3.857
Ni–Cl(1)	2.525(1)	Ni···Ni ^{II}	4.028
Ni–Cl(2)	2.392(1)		
N(1)–Ni–N(2)	77.9(1)	N(3)–Ni–Cl(1)	88.8(1)
N(1)–Ni–N(3)	97.7(2)	N(3)–Ni–Cl(2)	92.8(1)
N(1)–Ni–Cl(1)	85.1(1)	N(3)–Ni–Cl(2 ^I)	166.7(1)
N(1)–Ni–Cl(2)	168.9(1)	Cl(1)–Ni–Cl(2)	98.94(5)
N(1)–Ni–Cl(2 ^I)	90.4(1)	Cl(1)–Ni–Cl(2 ^I)	102.49(3)
N(2)–Ni–N(3)	82.9(1)	Cl(2)–Ni–Cl(2 ^I)	78.63(4)
N(2)–Ni–Cl(1)	159.8(1)	Ni–Cl(1)–Ni ^{II}	105.73(6)
N(2)–Ni–Cl(2)	99.8(1)	Ni–Cl(2)–Ni ^I	101.37(4)
N(2)–Ni–Cl(2 ^I)	88.6(1)	Ni–N(1)–N(1 ^{II})	131.5(1)

**Fig. 3** View of the molecular structure of the tetranuclear unit of complex **2a**. Details as in Fig. 2**Fig. 4** Part of the one-dimensional alternating chain structure of complex **2b**. Details as in Fig. 2

(trigonal bipyramidal). These findings seem surprising, as there is no obvious geometric or steric distinction between the two pyrazolate-bridged metal centres in a dinuclear framework like **1** that would restrict a possible increase in co-ordination number to only one of them. Indeed, simply the use of CH_2Cl_2 instead of CHCl_3 as the solvent for crystallisation induces the formation of polymeric one-dimensional alternating chains built from bimetallic pyrazolate complexes that are linked *via* dichloro bridges (**2b**). Compound **2b** crystallises in space group $C2/c$ with one half CH_2Cl_2 solvent molecule per nickel atom in the crystal lattice. A part of the chain structure of **2b** is shown in Fig. 4, selected bond lengths and angles are listed in Table 4.

A comparison of **2a** and **2b** reveals that the change in co-ordination number from five to six is accompanied by a significant lengthening of the mean nickel–ligand atom distances and an increase of the $\text{Ni}\cdots\text{Ni}$ separation within the basic pyrazolate-bridged skeleton [$d(\text{Ni}\cdots\text{Ni}) = 3.924$ (**2a**), 4.028 Å (**2b**)]. The bond lengths $\text{Ni}-\text{Cl}_{\text{bridge}}$ for the pyrazolate-based units are found to be $2.445(2)/2.439(2)$ Å in **1** *versus* $2.525(1)$ Å in **2b**, and bond lengths close to these values are also observed for the respective five-co-ordinate and six-co-ordinate nickel ions in the tetranuclear species **2a**, where the co-ordination number asymmetry thus gives rise to considerably different

atom distances $\text{Ni}(1)-\text{Cl}(2)$ [$2.536(1)$ Å] and $\text{Ni}(2)-\text{Cl}(2)$ [$2.435(1)$ Å]. Similar variations have previously been observed for a series of pyrazolate-bridged dinuclear complexes, in which the co-ordination number asymmetry was imposed by different chelating side arms in the 3- and 5-positions of the heterocycle.¹¹ Subtle modifications of the chelating side arms of a dinuclear pyrazolate ligand in conjunction with the choice of an appropriate solvent for crystallisation thus enable the construction of complexes with differing extents of aggregation, leading to either single bimetallic or oligomeric or even one-dimensional polymeric solid-state structures.

Magnetic properties of the complexes

The temperature-dependence of the magnetic susceptibilities for powdered samples of **1**, **2a** and **2b** is plotted in Fig. 5. The χ_m value is found to increase with decreasing temperature, reaching a maximum at around 35 K (**1**), 30 K (**2a**) or 25 K (**2b**) and then tending towards zero at lower temperatures, while the $\chi_m T$ vs. T curve continuously decreases upon cooling, this behaviour being indicative of overall antiferromagnetic coupling in all cases.

For the dinuclear complex **1** the experimental data have been fitted to the theoretical expression for the isotropic spin-Hamiltonian $H = -2J \cdot S_1 \cdot S_2$ (with $S_1 = S_2 = 1$) including a molar fraction p of uncoupled paramagnetic impurity [equation (1)]¹⁴ where N_a refers to the temperature-independent para-

$$\chi_m = [\chi_{m,\text{dim}}(1 - p)] + (2\chi_{m,\text{mono}}p) + 2N_a \quad (1)$$

magnetism [$100 \times 10^{-6} \text{ cm}^3 \text{ mol}^{-1}$ per nickel(II) ion¹]. $\chi_{m,\text{dim}} = (Ng^2\mu_B^2/kT) \cdot [2\exp(2J/kT) + 10\exp(6J/kT)] / [1 + 3\exp(2J/kT) + 5\exp(6J/kT)]$ and $\chi_{m,\text{mono}} = 2Ng^2\mu_B^2/3kT$, all other parameters have their usual meaning. Although powder measurements are not ideally suited for a thorough analysis of $S = 1$ dinuclear systems, the intradimer exchange term J often proved to be the dominant term in the spin-Hamiltonian.^{14,15} Accordingly, the experimental results for **1** are satisfactorily modelled despite the neglect of both a zero-field splitting parameter D and interdimer interactions $z'J'$, if data only down to 10 K are included in the fitting procedure. The best parameters obtained are $J = -13.5 \text{ cm}^{-1}$, $g = 1.96$ and $p = 2.9\%$ [agreement factor $R = \Sigma(\chi_m^{\text{calc}} - \chi_m^{\text{obs}})^2 / \Sigma(\chi_m^{\text{obs}})^2 = 3.1 \times 10^{-4}$], the value of J thus being in reasonable agreement with the exchange interactions observed in the range $8.1\text{--}13.1 \text{ cm}^{-1}$ for a series of related dinuclear nickel(II) complexes with both a pyrazolato and a chloro bridge.¹¹ The unusually low value of the g factor (being even smaller if no paramagnetic impurity is included) is probably due to zero-field splitting effects which were not taken into account.

To our knowledge no analytical expression for the magnetic properties of a linear Ni_4 complex with alternating bridges has hitherto been reported in the literature. In a preliminary approach, we employed the dimer model [equation (1)] for an analysis of the susceptibility data of **2a** [Fig. 5(b)] to obtain a good quality fit with $J = -11.1 \text{ cm}^{-1}$, $g = 2.12$ and $p = 3.5\%$ ($R = 5.5 \times 10^{-5}$). However, these values have to be interpreted with caution, as it cannot be assumed that the magnetic superexchange propagated by the dichloro linkage between the two bimetallic pyrazolate-based units is negligible, particularly in view of the results obtained for **2b**.

As expected, attempts to use equation (1) in order to adjust the experimental susceptibility data for compound **2b** only gave a poor fit ($J = -10.9 \text{ cm}^{-1}$, $g = 2.01$, $p = 4.0\%$; $R = 1.4 \times 10^{-3}$). Borrás-Almenar *et al.* recently reported analytical expressions for J -alternating chain systems with local spin $S = 1$ derived

from the Hamiltonian $H = -2J \sum_{i=1}^N (S_{2i} \cdot S_{2i+1} + aS_{2i} \cdot S_{2i-1})$ for

both cases of either overall antiferromagnetic (AF/AF)^{6a} or alternating antiferromagnetic/ferromagnetic (AF/F)^{6b} coupling, where the alternance parameter a relates the two nearest

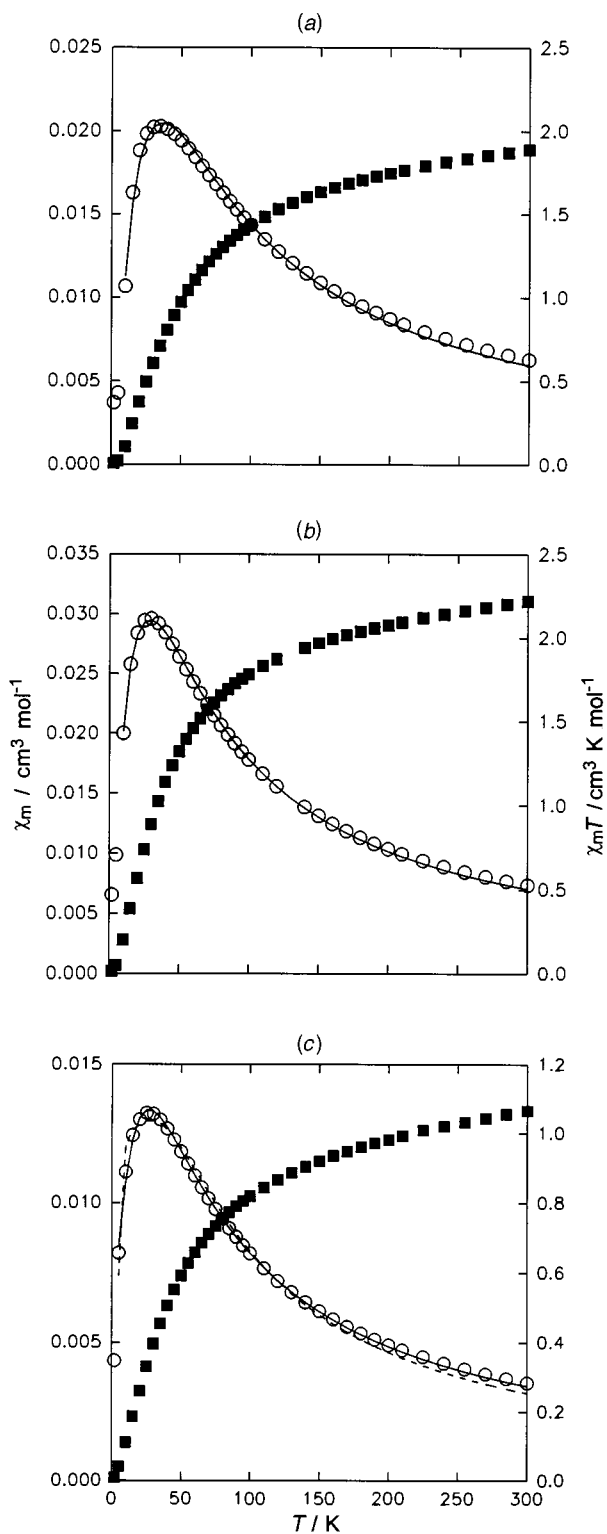


Fig. 5 Temperature-dependence of the magnetic susceptibilities for complexes (a) **1**; (b) **2a** (per dinuclear unit); (c) **2b** (per nickel ion). The solid line in each case represents the calculated curve. For complex **2b** the curves are calculated using the alternating chain equations⁶ with AF/AF coupling (—) and AF/F coupling (---) (see text)

neighbour exchange interactions and $2N$ is the number of interacting spins. Considering the results for **1** and **2a** as well as for the related dinickel(II) complexes described recently, in particular for a μ -chloro- μ -pyrazolato dinickel(II) compound with both metal ions in a distorted octahedral surrounding,¹¹ it can be assumed that antiferromagnetic coupling occurs within the pyrazolate-based dimeric cores. However, the type of magnetic exchange propagated *via* the dichloro bridges in **2b** is not known *a priori*, and thus both AF/AF and AF/F behaviour has

to be considered. By applying the expression for the AF/AF case^{6a} a good quality fit with optimised coupling parameters $J = -9.1 \text{ cm}^{-1}$, $g = 2.11$ and $aJ = -7.7 \text{ cm}^{-1}$ ($R = 1.9 \times 10^{-4}$) is obtained [solid line in Fig. 5(c)]. In view of the results mentioned above we assign the larger value of $J = -9.1 \text{ cm}^{-1}$ to the coupling within the basic pyrazolate-bridged unit. The obvious decrease of the magnitude of the magnetic exchange within the pyrazolate-based dinuclear core when going from five-coordinate (**1**: $J = -13.5 \text{ cm}^{-1}$) to mixed five/six-co-ordinate (**2a**: $J = 11.1 \text{ cm}^{-1}$) and overall six-co-ordinate nickel(II) ions (**2b**: $J = -9.1 \text{ cm}^{-1}$) is in accord with the observed trend for other μ -chloro- μ -pyrazolato dinickel systems with differing coordination numbers¹¹ and might be related to a more efficient orbital overlap for the five-co-ordinate species caused by the slightly shorter Ni-N_{pyrazolate} and Ni-Cl_{bridge} bond lengths (see above). Previous investigations on di- μ -chloro-bridged nickel(II) dimers^{16,17} have revealed antiferromagnetic behaviour in the case of five-co-ordinate *SPY-5* metal ions, but ferromagnetic superexchange for *TBPY-5* and six-co-ordinate metal ions. Attempts to model the experimental data for **2b** by the AF/F expression with optimised parameters $J = -12.6 \text{ cm}^{-1}$, $g = 1.96$ and $aJ = +9.1 \text{ cm}^{-1}$ however led to a clearly worse fit [$R = 6.4 \times 10^{-4}$; dashed line in Fig. 5(c)], thus suggesting a negative value for both J and aJ in the present case.

This latter choice is further corroborated when considering the above-mentioned trend in the magnitude of $|J|$, *i.e.* its expected decrease with increasing Ni-Cl bridge bond lengths within the pyrazolate-bridged dinickel(II) units. Additional support for the AF/AF situation stems from a ligand-field analysis of the solid-state UV/VIS data of **2b** with regard to the significantly different g values obtained from the two fitting procedures. A value $\Delta_{\text{oct}} \approx 8370 \text{ cm}^{-1}$ can be deduced from the ν_1 absorption band (Table 1), and a calculated Racah parameter $B \approx 863 \text{ cm}^{-1}$ then results from the consideration of an octahedral strong-field coupling scheme. Taking $15B = 15\,615 \text{ cm}^{-1}$ for the gaseous ion $\text{Ni}^{2+}({}^3\text{P})$,¹⁸ this leads to a nephelauxetic ratio β of 0.829. From the expression¹⁹ $\lambda = -0.27 \cdot B^2/Dq$ we calculated the spin-orbit coupling constant λ to be -240 cm^{-1} , which implies a reasonable reduction of 28% compared to the free ion value of -335 cm^{-1} .²⁰ Using the relationship $g = 2 - 8\lambda/10Dq$ a g value of 2.23 can thus be derived from the UV/VIS data, which is in reasonable agreement with the analysis of the magnetic measurements only if one assumes AF/AF behaviour.

This unexpected result of overall AF/AF superexchange may be rationalised on the basis of the specific geometric conditions for the di- μ -chloro-linkage in **2b** as revealed by the crystallographic analysis. As J results from the sum of an antiferromagnetic contribution J_{AF} mainly dependent on the overlap integral between two magnetic orbitals centred on each metal ion, and a ferromagnetic contribution J_{F} depending on the two-electron exchange integral, Kahn and co-workers¹⁷ pointed out that for angles Ni-Cl-Ni close to 90° the overlap integral becomes very small and J_{AF} is therefore expected to be weak whatever the Ni-Cl bond length may be. Accordingly, the bridging angles for the ferromagnetically coupled OC-6 dinickel(II) complexes reported in the literature were generally found in the range $92\text{--}97^\circ$.^{16,17} In contrast a considerably larger Ni-Cl(2)-Ni^I angle [$101.37(4)^\circ$] is observed for **2b**, indicating that in the present case J_{AF} might not vanish but play a dominant role and consequently lead to observable antiferromagnetic exchange coupling propagated *via* the di- μ -chloro-linkage. It should however be emphasised that additional factors, *e.g.* the pronounced asymmetry in the NiCl_2Ni framework of **2b** [$d[\text{Ni}-\text{Cl}(2)] = 2.392(1)$, $d[\text{Ni}-\text{Cl}(2')] = 2.592(1) \text{ \AA}$] and the severe distortion of the octahedral co-ordination sphere around the nickel(II) ions may also contribute to the specific magnetic properties of **2b**, and further work is definitely needed for a conclusive understanding of this type of alternating chain compound.

Table 5 Crystal data and refinement details for complexes **1**, **2a** and **2b**

	1	2a	2b
Formula	C ₁₇ H ₃₅ Cl ₃ N ₆ Ni ₂ ·2CHCl ₃	C ₁₅ H ₃₁ Cl ₃ N ₆ Ni ₂ ·2CHCl ₃	C ₁₅ H ₃₁ Cl ₃ N ₆ Ni ₂ ·CH ₂ Cl ₂
<i>M_r</i>	786.0	757.9	604.1
Crystal size/mm	0.40 × 0.30 × 0.30	0.40 × 0.30 × 0.20	0.30 × 0.30 × 0.30
Crystal system	Orthorhombic	Triclinic	Monoclinic
Space group	<i>Pbca</i>	<i>P</i> $\bar{1}$	<i>C2/c</i>
<i>a</i> /Å	19.308(2)	11.038(4)	17.950(3)
<i>b</i> /Å	13.031(2)	11.857(3)	13.374(2)
<i>c</i> /Å	25.771(2)	12.847(3)	13.277(2)
α /°		70.30(1)	
β /°		77.64(2)	130.70(1)
γ /°		86.96(3)	
<i>U</i> /Å ³	6484(1)	1546(1)	2416(1)
$\rho_{\text{calc}}/\text{g cm}^{-3}$	1.610	1.624	1.661
<i>Z</i>	8	1	4
<i>F</i> (000)	3216	768	1248
<i>T</i> /K	200	200	200
$\mu(\text{Mo-K}\alpha)/\text{mm}^{-1}$	1.925	2.015	2.127
Scan mode	ω	ω	ω
<i>hkl</i> Ranges	0–22, 0–15, 0–30	0–13, \pm 13, –14 to 15	–18 to 23, –9 to 17, –17 to 13
2θ Range/°	3.8–50.0	3.6–50.0	4.2–50.5
Measured reflections	5634	5606	2262
Observed reflections [<i>I</i> > 2 σ (<i>I</i>)]	3535	4429	1966
Refined parameters	344	351	141
Maximum, minimum residual electron density/e Å ^{–3}	0.732, –0.809	0.715, 0.801	1.361, –1.267
<i>R</i> 1	0.059	0.037	0.044
<i>wR</i> 2 (refinement on <i>F</i> ²)	0.140	0.087	0.131
Goodness of fit	1.027	1.038	2.455

Conclusion

Bimetallic entities composed of dinucleating ligand systems that leave potentially accessible co-ordination sites at both co-ordinated metal centres are valuable building blocks for the formation of higher nuclearity complexes with alternating bridges. The extent of aggregation of the basic dinuclear units is varied by a fine-tuning of the primary ligand core and by the choice of appropriate conditions for crystallisation, yielding either a dinuclear, tetranuclear or infinite one-dimensional alternating chain compound of nickel(II) from the set of pyrazolate-based ligands employed in the present work. Temperature-dependent magnetic data reveal antiferromagnetic coupling between the nickel(II) centres for all the μ -chloro- μ -pyrazolato cores as well as for the di- μ -chloro-linkage of the alternating chain compound **2b**. The latter result, which contrasts the usual ferromagnetic superexchange in di- μ -chloro-bridged six-co-ordinate nickel(II), may stem from the specific geometric conditions observed in the solid-state structure of **2b**, in particular the unusually large bridging angle Ni–Cl–Ni. We plan to study further examples of these new types of *J*-alternating polynuclear complexes in order to enable a more conclusive understanding of their properties.

Experimental

All manipulations were carried out under an atmosphere of dry nitrogen by employing standard Schlenk techniques. Solvents were dried according to established procedures. The compound HL¹ was synthesised according to the reported method.⁹ Microanalyses: Mikroanalytische Laboratorien des Organisch-Chemischen Instituts der Universität Heidelberg; IR spectra: Bruker IFS 66 FTIR; FAB- and EI-MS spectra: Finnigan MAT 8230; UV/VIS/NIR spectra: Perkin-Elmer Lambda 19; magnetic measurements: Quantum Design SQUID magnetometer MPMS-5S; the sample device has been described recently.²¹ All susceptibility measurements were performed at 1, 10 and 20 kG (1 G = 10^{–4} T). The field-dependence of the data was found to be small, and the 10 kG data were used for further analyses.

Syntheses

HL². Pyrazole-3,5-dicarboxylic acid monohydrate (2.7 g, 15.5 mmol) was converted into 3,5-bis(chloroformyl)pyrazole by means of SOCl₂.¹² This was taken up in thf (150 ml) and a solution of 1-(dimethylamino)-2-(methylamino)ethane (5.8 ml, 45.6 mmol) and ethyl(diisopropyl)amine (8.0 ml, 45.9 mmol) in thf (80 ml) was added dropwise with stirring. The reaction mixture was left at room temperature overnight, then filtered and evaporated to dryness. The resulting crude oil was redissolved in thf (40 ml) and filtered again. After removal of all volatile material under vacuum 4.4 g (88%) of the bis(amide) remained as a yellowish oil, $\delta_{\text{H}}(\text{CDCl}_3)$ 2.27 (12 H, s, CH₃), 2.56 (4 H, m, CH₂), 3.05, 3.27 (4 H, 2s, br, *E*/*Z*-CONCH₃), 3.67 (4 H, m, CONCH₂) and 6.98 (1 H, s, pyrazole H⁴); $\delta_{\text{C}}(\text{CDCl}_3)$ 34.7, 37.8, 45.7, 45.9, 46.3 (CH₃), 46.9, 49.7, 56.7, 57.7 (CH₂), 110.4 (pyrazole C⁴), 142.5 (br, pyrazole C^{3/5}) and 163.5 (br, CO). A solution of the bis(amide) (4.3 g, 13.3 mmol) in thf (80 ml) was added dropwise to a stirred suspension of LiAlH₄ (2.0 g, 52.7 mmol) in thf (200 ml). After the addition was completed the reaction mixture was heated at reflux for 5 h, then stirred at room temperature overnight and finally, while cooling to 0 °C, it was carefully quenched with water (10 ml). All inorganic precipitates were separated by filtration and washed twice with thf (50 ml). The combined filtrates were evaporated to dryness and the resulting crude oil was redissolved in light petroleum (b.p. 40–60 °C) (50 ml) and filtered again. Evaporation of all volatile material under vacuum afforded 3.0 g (76%) of the product as a slightly yellow oil, $\tilde{\nu}_{\text{max}}/\text{cm}^{-1}$ 3189m (br), 2944–2769s, 1575w, 1463s, 1123m and 1030s (film); $\delta_{\text{H}}(\text{CDCl}_3)$ 2.25 (12 H, s, CH₃), 2.30 (6 H, s, CH₃), 2.48 (8 H, m, CH₂), 3.62 (4 H, s, CH₂) and 6.70 (s, 1 H, CH); $\delta_{\text{C}}(\text{CDCl}_3)$ 43.2 (CH₃), 46.0 (CH₃), 54.4 (CH₂), 55.0 (CH₂), 57.8 (CH₂), 104.3 (pyrazole C⁴) and 146.2 (pyrazole C^{3/5}); *m/z* 296 (*M*⁺, 14%), 238 (*M*⁺ – CH₂NMe₂, 80), 195 [*M*⁺ – MeN(CH₂)₂NMe₂, 98] and 58 (CH₂NMe₂²⁺, 100).

Complex 1. A solution of HL¹ (0.26 g, 0.80 mmol) in EtOH (20 ml) was treated with NiCl₂·6H₂O (0.38 g, 1.60 mmol) and ethyl(diisopropyl)amine (0.16 ml, 0.92 mmol) and the resulting

light green solution was stirred at room temperature for 2 h while a precipitate formed. The volume of the reaction mixture was then reduced to ≈ 10 ml under vacuum and stirred for a further 5 h at 0 °C. Finally the solid was filtered off, washed with cold EtOH and dried under vacuum to yield 0.25 g (0.46 mmol, 57%) of light green $\text{Ni}_2\text{L}^1\text{Cl}_3$. Crystals of **1** were obtained by layering a solution of the complex in CHCl_3 with light petroleum (Found: C, 37.45; H, 6.55; Cl, 19.56; N, 15.46. $\text{C}_{17}\text{H}_{35}\text{Cl}_3\text{N}_6\text{Ni}_2$ requires C, 37.31; H, 6.45; Cl, 19.43; N, 15.36%); $\tilde{\nu}/\text{cm}^{-1}$ 2974w, 2905, 2862m, 1514w, 1469s, 1312m, 1199m, 1033s, 976m, 826s, 762s and 506w; m/z 511 ($M^+ - \text{Cl}$, 100%).

Complexes 2a and 2b. A solution of HL^2 (0.17 g, 0.58 mmol) in EtOH (20 ml) was treated with $\text{NiCl}_2 \cdot 6\text{H}_2\text{O}$ (0.27 g, 1.14 mmol) and ethyl(diisopropyl)amine (0.11 ml, 0.63 mmol) and the resulting orange-yellow solution was stirred at room temperature for 3 h. The volume of the reaction mixture was then reduced to ≈ 7 ml under vacuum and cooled to -20 °C, causing the precipitation of a green-yellow solid. This was filtered off, washed with cold EtOH and dried under vacuum to yield 0.15 g (0.29 mmol, 50%) of $\text{Ni}_2\text{L}^2\text{Cl}_3$. Orange-yellow crystals of **2a** were obtained by layering a solution of the complex in CHCl_3 with light petroleum (Found: C, 29.42; H, 4.95; Cl, 33.70; N, 12.61. $\text{C}_{15}\text{H}_{31}\text{Cl}_3\text{N}_6\text{Ni}_2 \cdot \text{CHCl}_3$ requires C, 30.09; H, 5.05; Cl, 33.31; N, 13.16%); $\tilde{\nu}/\text{cm}^{-1}$ 2980m, 2887m, 1516w, 1460s, 1330m, 1029m, 1007m, 963m, 810m, 749s, 664m, 603w, 488m and 463w; m/z 483 ($\text{Ni}_2\text{L}^2\text{Cl}_2^+$, 100%). Layering a solution of the crude complex in CH_2Cl_2 with light petroleum afforded green crystals of **2b** (Found: C, 31.82; H, 5.31; Cl, 28.63; N, 13.88. $\text{C}_{15}\text{H}_{31}\text{Cl}_3\text{N}_6\text{Ni}_2 \cdot \text{CH}_2\text{Cl}_2$ requires C, 31.81; H, 5.51; Cl, 29.34; N, 13.91%); $\tilde{\nu}/\text{cm}^{-1}$ 2967w, 2881m, 1507w, 1454s, 1328s, 1263m, 1029m, 1007m, 963m, 809m, 774m, 728s, 698m, 600w, 487w and 461w.

Crystallography

Structure determinations. The measurements were carried out on a Siemens (Nicolet Syntex) R3m/v four-circle diffractometer with graphite-monochromated Mo-K α ($\lambda = 0.71073$ Å) radiation. All calculations were performed with a micro-VAX computer using the SHELXTL PLUS software package.²² Structures were solved by direct methods with the SHELXS 86 and refined with the SHELX 93 programs.²² An absorption correction (ψ scan, $\Delta\psi = 10^\circ$) was applied to all data. Atomic coordinates and anisotropic thermal parameters of the non-hydrogen atoms were refined by full-matrix least-squares calculations. The hydrogen atoms were placed at calculated positions and constrained to ride on the atoms they were attached to. Table 5 compiles the data for the structure determinations.

CCDC reference number 186/886.

See <http://www.rsc.org/suppdata/dt/1998/1181/> for crystallographic files in .cif format.

Acknowledgements

We are grateful to Professor Dr. G. Huttner for his generous and continuous support of our work as well as to the Deutsche Forschungsgemeinschaft (Habilitationstipendium for F. M.) and the Fonds der Chemischen Industrie for financial support. Professor Dr. H. Lueken and the DFG are sincerely thanked for allowing the use of the SQUID magnetometer.

References

- O. Kahn, *Molecular Magnetism*, VCH, Weinheim, 1993.
- Research Frontiers in Magnetochemistry*, ed. C. J. O'Connor, World Scientific, Singapore, 1993.
- E. Coronado, M. Drillon, A. Fuertes, D. Beltran, A. Mosset and J. Galy, *J. Am. Chem. Soc.*, 1986, **108**, 900; A. Escuer, R. Vicente and X. Solans, *J. Chem. Soc., Dalton Trans.*, 1997, 531.
- R. Vicente, A. Escuer, J. Ribas and X. Solans, *Inorg. Chem.*, 1992, **31**, 1726; A. Escuer, R. Vicente, M. S. El Fallah, J. Ribas, X. Solans and M. Font-Bardia, *J. Chem. Soc., Dalton Trans.*, 1993, 2975; A. Escuer, R. Vicente, J. Ribas, M. S. El Fallah, X. Solans and M. Font-Bardia, *Inorg. Chem.*, 1994, **33**, 1842; J. Ribas, M. Montfort, B. K. Gosh and X. Solans, *Angew. Chem., Int. Ed. Engl.*, 1994, **33**, 2077; J. Ribas, M. Montfort, B. K. Gosh, X. Solans and M. Font-Bardia, *J. Chem. Soc., Chem. Commun.*, 1995, 2375; R. Vicente and A. Escuer, *Polyhedron*, 1995, **14**, 2133.
- C. S. Hong, J. Kim, N. H. Hur and Y. Do, *Inorg. Chem.*, 1996, **35**, 5110.
- (a) J. J. Borrás-Almenar, E. Coronado, J. Curely and R. Georges, *Inorg. Chem.*, 1995, **34**, 2699; (b) J. J. Borrás-Almenar, J. Clemente-Juan, E. Coronado and F. Lloret, *Chem. Phys. Lett.*, 1997, **275**, 79.
- A. Escuer, R. Vicente, X. Solans and M. Font-Bardia, *Inorg. Chem.*, 1994, **33**, 6007.
- G. Viau, M. G. Lombardi, G. De Munno, M. Julve, F. Lloret, J. Faus, A. Caneschi and J. M. Clemente-Juan, *Chem. Commun.*, 1997, 1195.
- F. Meyer, S. Beyreuther, K. Heinze and L. Zsolnai, *Chem. Ber./Recl.*, 1997, **130**, 605.
- F. Meyer, K. Heinze, B. Nuber and L. Zsolnai, *J. Chem. Soc., Dalton Trans.*, 1998, 207; F. Meyer, A. Jacobi, B. Nuber, P. Rutsch and L. Zsolnai, *Inorg. Chem.*, in the press.
- M. Konrad, F. Meyer, K. Heinze and L. Zsolnai, *J. Chem. Soc., Dalton Trans.*, 1998, 199.
- C. Acerete, J. M. Bueno, L. Campayo, P. Navarro and M. I. Rodriguez-Franco, *Tetrahedron*, 1994, **50**, 4765.
- (a) M. Ciampolini, N. Nardi and G. P. Speroni, *Coord. Chem. Rev.*, 1966, **1**, 222; (b) C. Furlani, *Coord. Chem. Rev.*, 1968, **3**, 141; (c) D. Nicholls, in *Comprehensive Inorganic Chemistry*, eds. J. C. Bailar, H. J. Emeléus, R. Nyholm and A. F. Trotman-Dickenson, Pergamon, Oxford, 1973, 1st edn., vol. 3, p. 1152 ff.
- C. J. O'Connor, *Prog. Inorg. Chem.*, 1982, **29**, 203.
- P. Chauduri, H.-J. Küppers, K. Wiegardt, S. Gehring, W. Haase, B. Nuber and J. Weiss, *J. Chem. Soc., Dalton Trans.*, 1988, 1367.
- A. P. Ginsberg, R. L. Martin, R. W. Brookes and R. C. Sherwood, *Inorg. Chem.*, 1972, **11**, 2884; C. G. Barraclough and R. W. Brookes, *J. Chem. Soc., Faraday Trans.*, 1974, **70**, 1364; E. J. Laskowski, T. R. Felthouse, D. N. Hendrickson and G. J. Long, *Inorg. Chem.*, 1976, **15**, 2908; R. J. Butcher, C. J. O'Connor and E. Sinn, *Inorg. Chem.*, 1979, **18**, 492; K. O. Joung, C. J. O'Connor, E. Sinn and R. L. Carlin, *Inorg. Chem.*, 1979, **18**, 804; J. C. Jansen, H. van Koningsveld, J. A. C. van Ooijen and J. Reedijk, *Inorg. Chem.*, 1980, **19**, 170; C. P. Landee and R. D. Willett, *Inorg. Chem.*, 1981, **20**, 2521.
- I. Bkouche-Waksman, Y. Journaux and O. Kahn, *Transition Met. Chem.*, 1981, **6**, 176.
- J. Huheey, E. Keiter and R. Keiter, *Anorganische Chemie*, Walter de Gruyter, Berlin, 2nd edn., 1995, p. 517.
- J. Reedijk, P. W. N. M. van Leeuwen and W. L. Groeneveld, *Recl. Trav. Chim. Pays-Bas*, 1968, **87**, 129.
- I. B. Bersuker, *Electronic Structure and Properties of Transition Metal Ions*, Wiley Interscience, New York, 1996, p. 37.
- P. Wehausen, O. Borgmeier, A. Furrer, P. Fischer, P. Allenspach, W. Henggeler, H. Schilder and H. Lueken, *J. Alloys Compd.*, 1997, **246**, 139.
- G. M. Sheldrick, SHELXTL PLUS, Program Package for Structure Solution and Refinement, Siemens Analytical Instruments, Madison, WI, 1990; SHELX 93, Program for Crystal Structure Refinement, Universität Göttingen, 1993; SHELXS 86, Program for Crystal Structure Solution, Universität Göttingen, 1986.

Received 27th November 1997; Paper 7/08565F